

# EFFECT OF DEFORMATION ON SENSITISATION PROCESS IN AUSTENITIC STAINLESS STEEL AISI 316

Mária DOMÁNKOVÁ<sup>1</sup>, Edina KOCSISOVÁ<sup>1</sup>, Peter PINKE<sup>2</sup>,  
Ivan SLATKOVSKÝ<sup>1</sup>

*Authors:* Assoc. Prof. Ing. Mária Dománková, PhD. <sup>1</sup>, Ing. Edina Kocsisová<sup>1</sup>,  
Ing. Peter Pinke, PhD. <sup>2</sup>, Ing. Ivan Slatkovský<sup>1</sup>

*Workplace:* <sup>1</sup>Institute of Materials Science, Faculty of Materials Science and  
Technology, Slovak University of Technology  
<sup>2</sup> Detached workplace Komárno

*Phone:* +421 0906 068 509, 0906 068 531

*Address:* <sup>1</sup>Bottova 25, 917 24, Trnava  
<sup>2</sup> Senný trh 6, 945 01 Komárno

*Email:* [maria.domankova@stuba.sk](mailto:maria.domankova@stuba.sk), [edina.kocsisova@stuba.sk](mailto:edina.kocsisova@stuba.sk)  
[peter.pinke@stuba.sk](mailto:peter.pinke@stuba.sk), [ivan.slatkovsky@stuba.sk](mailto:ivan.slatkovsky@stuba.sk)

## Abstract

*The process of the secondary phases' precipitation controls the mechanical and physical properties of the stainless steels. The aim of this study is characterisation of the selected factors (temperature expositions and deformation) influencing kinetics of the secondary phases' precipitation at the grain boundaries. The effect of uniaxial deformation 20, 30 and 40% on the degree of sensitisation (DOS) in AISI 316 austenitic stainless steel was investigated in the temperature range from 500 to 900 °C with the aging time in the interval 0.1 to 1000 h. The results showed that the deformation accelerated the sensitisation process. Transmission electron microscopy was used to identify the secondary phases which precipitated on the grain boundaries.*

## Key words

*austenitic stainless steel, sensitisation, precipitation, transmission electron microscopy, corrosion.*

## Introduction

Stainless steels (SSs) are characterised by the chemical composition which guarantees their corrosion resistance in various working environments. These materials contain relatively high content of expensive alloying elements, and their production is very expensive and energy-consuming. Their application has to be rational and economical. For the correct steels selection, it is necessary to have information of their properties with the respect to the construction and conditions of their application (1-3).

Austenitic stainless steels (ASSs) have a dominant position in the group of SSs. Austenitic stainless steels are the most favoured construction materials of various components required in the chemical, petrochemical and nuclear industries. The selection of these is based on a good combination of mechanical, fabrication and corrosion resistance properties. The exposition in the temperature range of 500-800°C leads to the precipitation of  $M_{23}C_6$  chromium-rich carbide on the grain boundary and to the formation of the chromium depletion regions. If the chromium content near the grain boundaries drops under the passivity limit 12 wt. %, the steel becomes to be sensitised (1-4). In the sensitised condition, the steels are quite susceptible to the intergranular corrosion (IGC) and intergranular stress corrosion cracking (IGSCC) that can result in premature failures of the fabricated components. The sensitisation temperature range is often encountered during isothermal heat treatment, slow cooling from the solution annealing temperature, improper heat treatment in the heat affected zone of the welds or weld joints or hot working of the material. Degree of the sensitisation (DOS) is influenced by the factors such as the steel chemical composition, grain size, degree of strain, or temperature and time of isothermal annealing (5-7).

Sensitisation resulting from isothermal exposure is normally represented by time-temperature-sensitisation (TTS) diagrams which are plots of aging time versus the temperature necessary for sensitisation. These are “C” shaped curves, which separate the sensitised and non-sensitised regions. The TTS diagrams show the time required for isothermal sensitisation at various temperatures and can be used to solve the problems such as the selection of conditions of annealing which will not result in sensitisation. The nose of this curve specifies the critical temperature at which the minimum time ( $t_{min}$ ) is required for sensitisation (3, 8).

Effects of annealing and plastic deformation on ASSs are mostly considered as a complex phenomenon of the synergetic nature. As an example, the process of thermo-mechanical treatment which affects the optimisation of the ASS mechanical properties can be used. Study of the plastic deformation influence on sensitisation of ASSs is concentrated on the detailed analysis of the material texture, misorientation and distribution character of the grain boundary. The influence of the degree of strain on the position of “C” curves and the critical linear cooling rate was proved (2, 3, 8).

In this research article, we report on some preliminary comparisons of the combined effects of deformation, temperature and aging time on sensitisation in AISI 316 austenitic stainless steel.

## **Experimental steel and procedures**

### ***Material, heat treatment and cold working***

The chemical composition of experimental steel is given in Table 1. The material examined was supplied in the condition after solution annealing (1050 °C for 60 min), followed by water quenching.

CHEMICAL COMPOSITION (in wt. %) OF AUSTENITIC STAINLESS STEEL USED  
IN THIS STUDY

Table 1

steel	C	N	Si	Mn	P	S	Cr	Ni	Mo	Fe
AISI 316	0.05	0.032	0.47	0.86	0.0026	0.001	17.55	11.56	2.10	bal.

The steels were cold rolled ranging from 20 to 40% by controlling the thickness of plates. The degree of cold work (CW) was used to express the reduction ration in thickness. The specimens of 15 mm length and 8 mm width with reduced thickness were cut from the cold rolled strips for sensitisation testing. The cold worked samples were heat treated at various temperatures range from 500 – 900 °C for duration range from 0.1 to 1000 hrs. The samples were water quenched after the heat treatments.

### *Specimen preparation*

The specimens for microstructure analysis were mounted in an epoxy resin and were polished up to fine diamond (~1µm) finish. The specimens were etched electrolytically, using 5 % oxalic acid solution for microstructural characterisation.

### *Sensitisation test*

To determine the steel's sensitivity to intergranular corrosion, an oxalic acid etched test (ASTM A262 practice A) was used. The specimens were electrolytically etched in 10% oxalic acid for 90 sec. at a current density of 1 A/cm<sup>2</sup>. The etched structure is then examined at 250 x and was characterised as the step, dual or ditch structure. The specimen showing the step or dual structure was considered to be free from sensitisation, whereas the specimen showing the ditch structure was classified as sensitised (9).

### *Construction of the time-temperature-sensitisation diagrams*

These diagrams were obtained by plotting the sensitisation test results on a temperature versus the log soaking time axes and drawing a line which demarcates the sensitised and non-sensitised regions.

### *Phase identification*

For individual secondary phase identification, transmission electron microscopy (TEM) of extraction carbon replicas was utilised. TEM observations were performed using JEOL 200 CX operated at 200 kV. Carbon extraction replicas were obtained from mechanically polished and etched surfaces. The replicas were stripped from the specimens in solution of CH<sub>3</sub>COOH : HClO<sub>4</sub> = 4 :1 at 20 °C, 15 V. The analysis was supplemented by the selected area electron diffraction and EDS for phase identification of the small particles on grain boundaries.

## Results

### *Microstructural characterisation*

The results of light microscopy investigation are summarised in Fig.1. Microstructure of AISI 316 after solution annealing is composed of polyhedral austenitic grains with twinning typical for fcc structure. The average austenitic grain size of this state is about  $40\pm 8\ \mu\text{m}$  (Fig. 1a). The small amount of  $\delta$ -ferrite was also recorded. No precipitates were observed at the grain boundaries (GB) of the solution annealed steels. Fig. 1b shows the microstructure of AISI 316 in the 40% CW condition. The microstructure is of a deformation texture, and the increased density deformation twins inside the austenitic grains were observed. Microstructure of the aged states is documented in Figs.1c and 1d. Fig.1c shows the evolution of the secondary phases' precipitation at the GB in the isothermally aged specimen ( $650\ ^\circ\text{C}/300\ \text{h}$ ) and 0%CW. The microstructure of the isothermally aged specimen ( $650\ ^\circ\text{C}/1000\ \text{h}$ ) and 40% CW is showed in Fig. 1d. Precipitation of secondary phases was observed at the GB and intragranularly within the matrix, too.

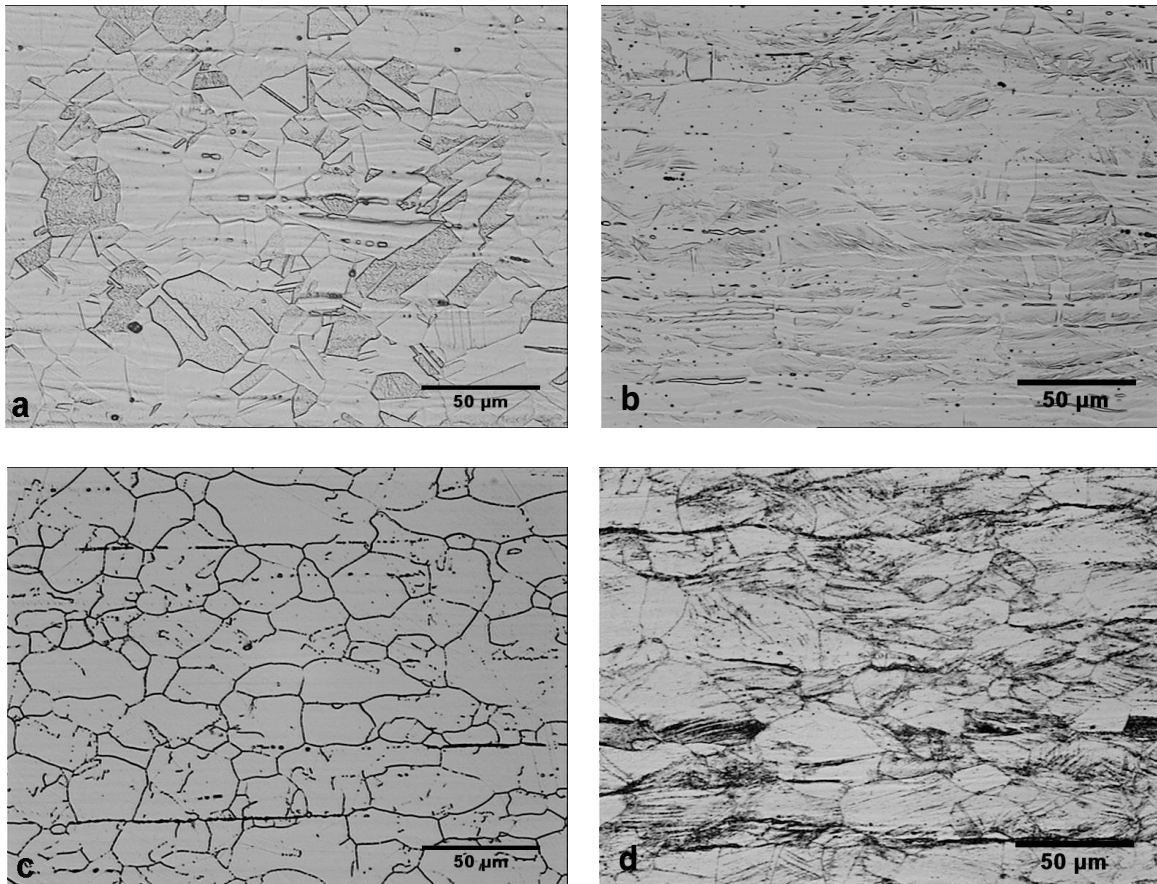


**Fig. 1** Microstructure of the experimental steel observed by light microscopy: a) after solution annealing (0% CW), b) after solution annealing (40% CW), c) after heat treatment  $650\ ^\circ\text{C}/300\ \text{h}$  (0% CW), d) after heat treatment ( $650\ ^\circ\text{C}/1000\ \text{h}$  (40%CW)

## *Corrosion behaviour*

The rapid oxalic acid etch test was used to analyse the grain boundary sensitisation development. The examples of microstructure obtained by etch test for experimental steels are given in Fig. 2. TTS diagrams were obtained by plotting the sensitisation test results on a temperature versus log soaking time axes and drawing a line which demarcates the sensitised and non-sensitised regions (Fig. 3). The nose of the curve for the experimental steel AISI 316 (0%CW) was at the temperature 800 °C and  $t_{\min}=20$  min. In the case of experimental steel AISI 316 (40%CW), the nose of the curve was at the temperature 800 °C and  $t_{\min}=6$  min. It demonstrated that cold working of the steel caused the shift of the critical part of TTS diagram (the nose of the curve) towards lesser time than 0% CW material.

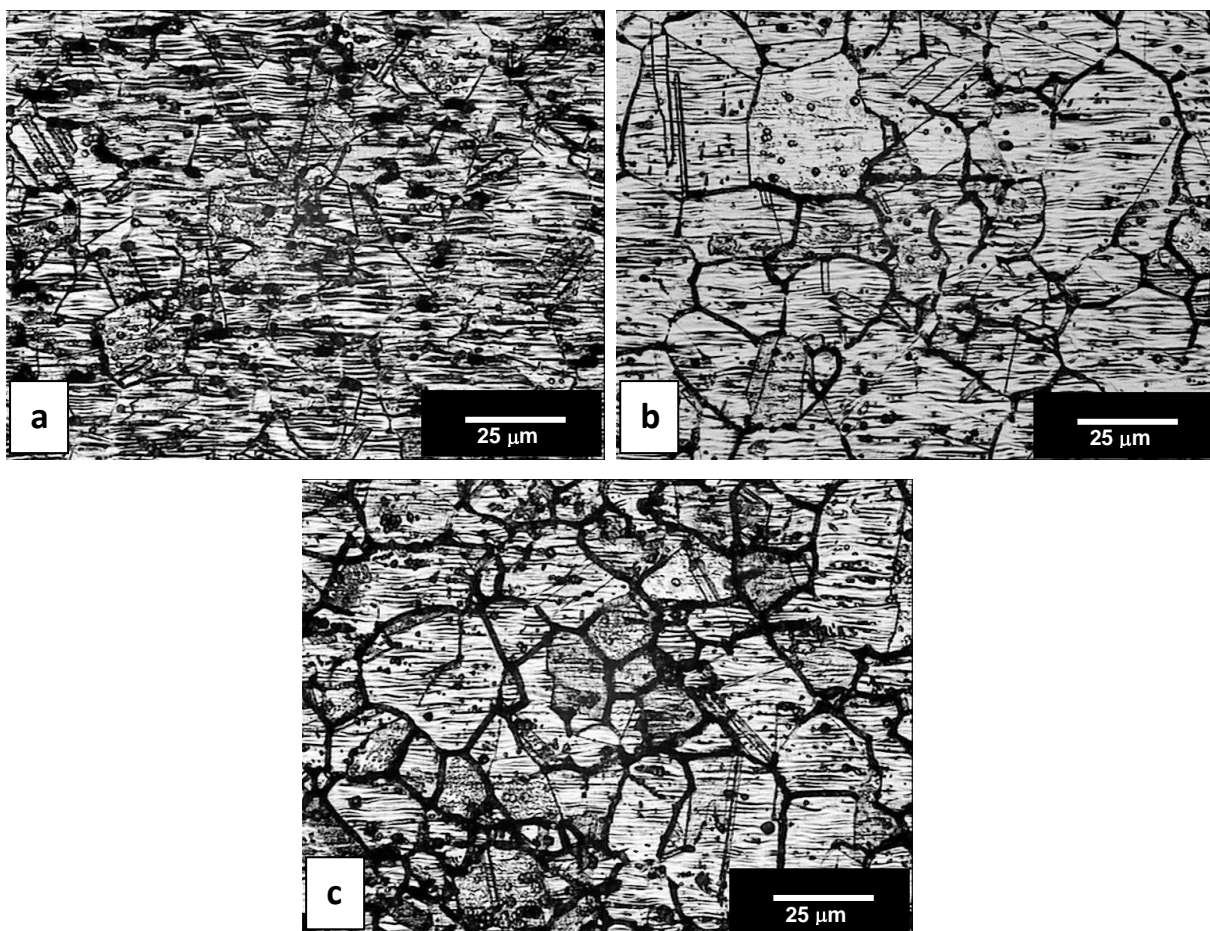


**Fig. 2** Examples of AISI 316 (0%CW) microstructure obtained after oxalic acid etch test a) after solution annealing (step), b) after aging 800 °C/10 min. (dual), c) after aging 800 °C/10 h (ditch)

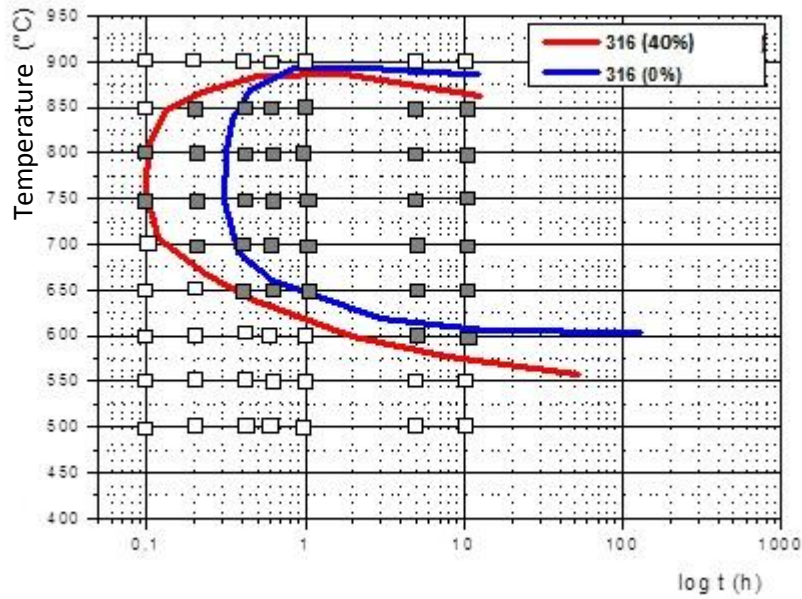


**Fig. 3** TTS diagrams for AISI type 316 (0%CW) and 316 (40%) austenitic stainless steels established as per ASTM A262 practice A test

□ non-sensitised, ■ sensitised

### ***Analysis of precipitation by TEM***

The TEM microstructure analysis was focused especially on the identification of the secondary phases which precipitated at the grain boundaries during the annealing. The changes of chemical composition and the relative size of particles were evaluated. Fig.4 shows the microstructure of AISI 316 (40%CW) in the solution annealing state observed by TEM. The pure grain boundaries are documented by the figure. Fig. 5 shows typical GBs formed in an early stage of the aging treatment (650 °C/10 min.); no particles of secondary phases were observed on GB using TEM, but some small particles were observed inside the austenitic grain on the slip lines. Fig.6 shows a detail of the grain boundary of AISI 316 (0%CW), where small particles of irregular shape can be observed. These particles were identified by electron diffraction as carbide  $M_{23}C_6$ . In the case of the experimental steel with 0% CW, the precipitation of secondary phases was observed only at the grain boundaries. First,  $M_{23}C_6$  carbide on the grain boundaries was detected after aging. Besides  $M_{23}C_6$  carbides,  $\sigma$ -phase and  $M_6C$  carbide were detected at the grain boundaries. Table 3 summarised the average metal composition and frequency (Fig. 7) of the identified secondary phases in AISI 316 (40%CW) steel after the aging treatment.

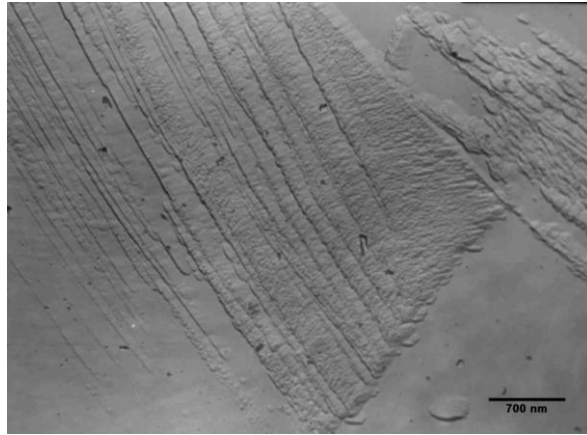


**Fig. 4** Microstructure of AISI 316 (40%CW) in the solution annealing state

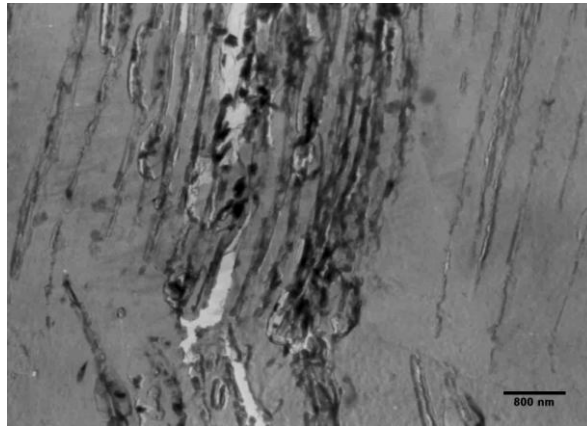


**Fig. 5** Microstructure of AISI 316 (40% CW) after heat treatment 650 °C/10 min

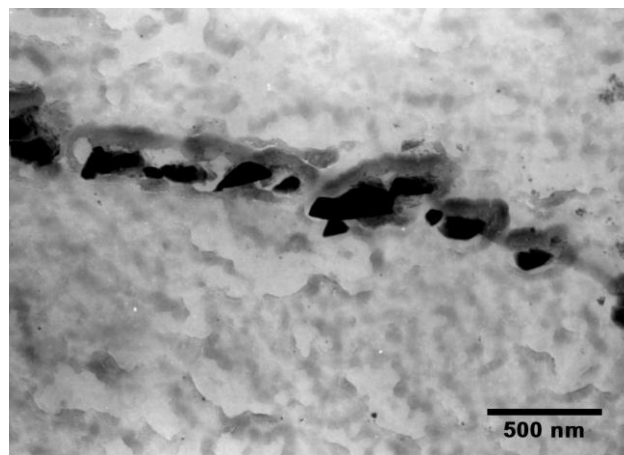


**Fig. 6** Detail of the grain boundary with particles of irregular shape after aging 750 °C/5 h in AISI 316 (0% CW)

AVERAGE METAL COMPOSITION IN wt. % OF IDENTIFIED SECONDARY PHASES  
IN AISI 316 (40%CW) STEEL AFTER AGING TREATMENT

Table 3

aging treatment	phase	metal composition (wt%)				frequency (%)
		Cr	Fe	Ni	Mo	
650°C/5 h	M <sub>23</sub> C <sub>6</sub>	64.1	19.4	1.8	14.7	72
	M <sub>6</sub> C	21.3	29.6	0.4	48.7	11
	σ-phase	19.6	59.7	0.8	19.9	17
650°C/10 h	M <sub>23</sub> C <sub>6</sub>	61.7	19.5	1.0	17.8	68
	M <sub>6</sub> C	14.5	30.2	0.8	54.4	15
	σ-phase	18.6	60.3	1.2	19.9	17
650°C/30 h	M <sub>23</sub> C <sub>6</sub>	64.7	20.1	0.0	15.2	51
	M <sub>6</sub> C	11.1	27.6	0.8	60.5	41
	σ-phase	24.2	59.3	3.1	13.4	8
650°C/100 h	M <sub>23</sub> C <sub>6</sub>	61.4	18.1	1.6	18.9	42
	M <sub>6</sub> C	13.6	30.6	1.3	54.5	54
	σ-phase	26.3	57.3	3.0	13.4	4
650°C/1000 h	M <sub>23</sub> C <sub>6</sub>	72.9	16.1	0.2	10.8	21
	M <sub>6</sub> C	9.6	29.4	1.7	59.3	75
	σ-phase	23.3	68.5	6.0	2.2	4

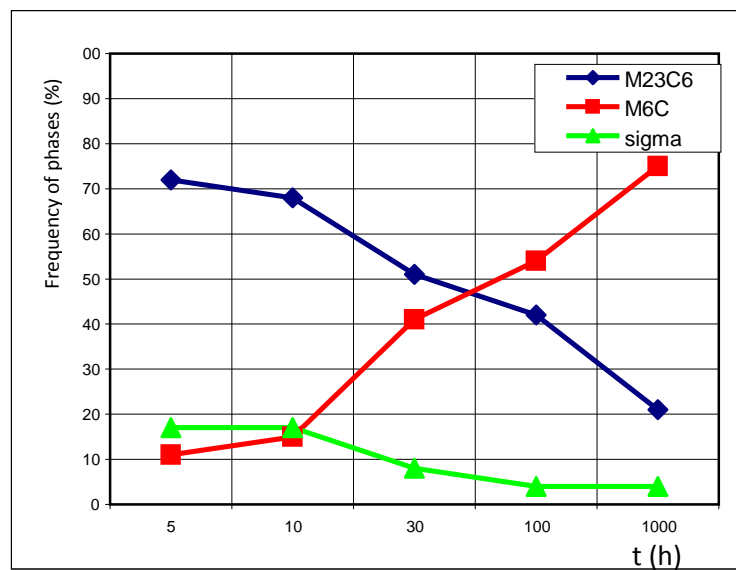


Fig. 7 Frequency of secondary phases in AISI 316 (40%CW) after aging at temperature 650 °C

## Conclusions

The precipitation behaviour of AISI 316 with 0%CW and 40%CW austenitic stainless steels was investigated at the aging at various temperatures range from 500 to 900 °C for duration range from 0.1 to 1000 hrs. The following conclusions were drawn:

1. TTS diagrams of the experimental steels after the oxalic acid etch test ASTM A262 practice A were constructed. It was demonstrated that C-curve of TTS diagrams are displaced towards lesser time by increasing the cold work,
2. After~40% cold working, even the sites inside the grain matrix have high energy, and carbides can nucleate there easily. Cold work increases the number of dislocations/dislocation pipes, along which diffusion rate of chromium is very high,
3. Sensitisation of the experimental steels accelerated the precipitation of the  $M_{23}C_6$  carbide; besides,  $M_{23}C_6$  carbide,  $\sigma$ -phase and  $M_6C$  carbide were also detected on the grain boundaries and in the austenitic matrix in the case of cold working samples.

## References:

1. LO, K.K., SHEK, C.H., LAI, J.K.L. 2009. Recent development in stainless steels. *Materials Science and Engineering:R:Reports*, 65, pp. 39-104.
2. PARVATHAVARTINI N., DAYAL R.K. 2002. Influence of chemical composition, prior deformation and prolonged thermal aging on sensitisation characteristics of austenitic stainless steels. *Journal of Nuclear Materials*, Vol.305, pp. 209-219.
3. TRILLO E.A., MURR L.E. 1999. Effects of carbon content, deformation and interfacial energetics on carbide precipitation and corrosion sensitisation in 304 stainless steel. *Acta Materialia*, Vol. 47 No.1, pp. 235-245.
4. TAVARES, S.S.M., MOURA, V., DA COSTA, V.C., FERREIRA, M.L.R., PARDAL, J.M. 2009. Microstructural changes and corrosion resistance of 310S steel exposed to 600-800 °C. *Material Characterization*, 60, pp. 573-578.
5. NISHIMURA R., MAEDA Y. 2003. Stress corrosion cracking of sensitised type 316 austenitic stainless steel in chloric acid solution-effect of sensitising time. *Corrosion Science*, Vol. 42, pp. 1847-1862.
6. WASNIK D.N., KAIN V., SAMAJDAR I. 2002. Resistance to sensitisation and intergranular corrosion through extreme randomisation of grain boundaries. *Acta Materialia*, Vol. 50, pp. 4587-4601.
7. SANZAY, M., BARARD, K., KARLEN, W. 2010. TEM observation and finite element modelling of channel deformation in pre-irradiated austenitic stainless steels – Interactions with the surfaces and grain boundaries. *Journal of Nuclear Materials*, 406, pp. 152-165.
8. MURR L.E. ADVANI A., SHAKAR S., ATTERIDGE D.G. 1990. Effects of deformation and heat treatment on grain boundary sensitisation and precipitation in austenitic stainless steels. *Material Characterization*, Vol. 24, pp.135-158.
9. ASTM standard practice in A 262 for detecting susceptibility to intergranular corrosion in austenitic stainless steels

## Reviewers:

Assoc. Prof. Ing. Ľubomír Čaplovič, PhD. – Institute of Materials Science, Faculty of Materials Science and Technology STU in Trnava

Prof. Ing. Frantisek Janiček, PhD. – Faculty of Electrical Engineering and Information Technology, STU Bratislava

## Acknowledgement

This publication is the outcome of the project: “Increase of Power Safety of the Slovak Republic” (ITMS: 262220220077) supported by the Research & Development Operational Programme funded by the ERDF



We support research activities in Slovakia. The project is co-financed by the EU.